Air-Parcel Residence Times Within Forest Canopies

Authors: Tobias Gerken, Marcelo Chamecki, and Jose D. Fuentes

The final publication is available at Springer via http://dx.doi.org/10.1007/s10546-017-0269-7 in Boundary Layer Meteorology.

Gerken, Tobias, Marcelo Chamecki, and Jose D. Fuentes. "Air-Parcel Residence Times Within Forest Canopies." Boundary Layer Meteorology (June 2017): 1-26.
DOI: 10.1007/s10546-017-0269-7.

Air-Parcel Residence Times Within Forest Canopies

Tobias Gerken[1,2] · **Marcelo Chamecki**[3] · **Jose D. Fuentes**[1]

Abstract We present a theoretical model, based on a simple model of turbulent diffusion and first-order chemical kinetics, to determine air-parcel residence times and the out-of-canopy export of reactive gases emitted within forest canopies under neutral conditions. Theoretical predictions of the air-parcel residence time are compared to values derived from large-eddy simulation for a range of canopy architectures and turbulence levels under neutral stratification. Median air-parcel residence times range from a few sec in the upper canopy to approximately 30 min near the ground and the distribution of residence times is skewed towards longer times in the lower canopy. While the predicted probability density functions from the theoretical model and large-eddy simulation are in good agreement with each other, the theoretical model requires only information on canopy height and eddy diffusivities inside the canopy. The eddy-diffusivity model developed additionally requires the friction velocity at canopy top and a parametrized profile of the standard deviation of vertical velocity. The theoretical model of air-parcel residence times is extended to include first-order chemical reactions over a range of of Damköhler numbers (Da) characteristic of plant-emitted hydrocarbons. The resulting out-of-canopy export fractions range from near 1 for $Da = 10^{-3}$ to less than 0.3 at $Da = 10$. These results highlight the necessity for dense and tall forests to include the impacts of air-parcel residence times when calculating the out-of-canopy export fraction for reactive trace gases.

✉ Tobias Gerken
tobias.gerken@montana.edu

Marcelo Chamecki
chamecki@ucla.edu

[1] Department of Meteorology and Atmospheric Sciences, The Pennsylvania State University, University Park, PA 16802, USA

[2] Present Address: Department of Land Resources and Environmental Sciences, Montana State University, Bozeman, MT 59717, USA

[3] Department of Atmospheric and Oceanic Sciences, University of California, Los Angeles, CA 90095, USA

1 Introduction

Forests cover large areas of the Earth's surface and play a key role in the exchange of momentum, energy, carbon dioxide, and reactive trace gases, such as biogenic volatile organic compounds (BVOCs). BVOCs principally include isoprene, monoterpenes, sesquiterpenes, and oxygenated species. BVOCs emitted into the canopy air space are subject to turbulent transport within forest canopies and undergo chemical reactions with atmospheric oxidants (e.g., Fuentes et al. 2000). For compounds with higher reactivities, such as β-caryophyllene or many monoterpenes, chemical lifetimes are comparable to the turbulent transport time scale within forest canopies, leading to significant chemical destruction inside the canopy (e.g, Stroud et al. 2005; Fuentes et al. 2007; Jardine et al. 2011; Rinne et al. 2012). Thus, estimates of within-canopy chemical reactions are needed when scaling leaf-level BVOC emissions to regional or global scales using numerical models such as the Model of Emissions of Gases and Aerosols from Nature (MEGAN; Guenther et al. 2006, 2012). Similarly, the net export of BVOC reaction products from forest canopies should be considered. Hereafter, we refer to the ratio between the emission flux and the flux at the top of the canopy as the export fraction.

The problem of estimating the export fraction can be intuitively described in a Lagrangian framework. One can imagine an air parcel passing through the source of BVOC inside the forest, then following its trajectory determined by the turbulent eddies, and eventually leaving the forest. The total chemical loss between the two points (release location and top of the canopy) depends on the reaction time scale τ_{chem} and the travel time inside the canopy τ_{turb}, usually termed the air-parcel residence time (Strong et al. 2004). Thus, one can model the chemical loss and the export fraction (sometimes referred to as the flux-to-emission ratio) in terms of the canopy Damköhler number defined as $Da \equiv \tau_{\text{turb}}/\tau_{\text{chem}}$ (Damköhler 1940).

In devising a model for the export fraction, one needs to extend the information on ambient oxidant concentrations that react with BVOCs and associated kinetics into τ_{chem} (e.g. Finlayson-Pitts 2000), and the information on turbulence characteristics and transport within plant canopies into τ_{turb}. The former is a difficult task given the complexity of the chemical reactions taking place inside the forest, and the latter is a difficult task due to the challenges in modelling turbulence in plant canopies (e.g. Finnigan 2000). In the present study, we focus on the issues of defining and modelling τ_{turb}, and we adopt a simple model for the chemistry with the goal of illustrating the importance of the residence times to the coupled chemistry-transport problem.

Starting from the mid 1990s, turbulence research has emphasized the importance of coherent mixing-layer eddies for the vertical transport of momentum and trace gases within forest canopies (e.g. Raupach et al. 1996; Finnigan 2000). The canopy structure (characterized by the leaf area index, LAI, and vertical leaf area density) influences the penetration depth of mixing-layer eddies into the forest canopy. Interactions of eddies with dense forests result in the canopy exhibiting two regions of distinct vertical transport. The upper region of the canopy is constantly flushed by strong and coherent mixing-layer eddies that adhere to a shear length scale and are efficient in transporting air parcels out of the canopy. Deep within canopies, small-scale wake turbulence dominates the trans-

port process and as a consequence forests act to shield air parcels from mixing with the airflow aloft. Therefore, scalar transport in canopies is strongly affected by source-sink distributions (e.g. Coppin et al. 1986; Iwata et al. 2010; Edburg et al. 2012) and one expects the export fraction to be strongly dependent on the source distribution as well.

The first studies that attempt to quantify the statistics of residence times and/or export fractions for BVOCs used Lagrangian stochastic models (LSMs) coupled to simple chemical reactions (Strong et al. 2004; Fuentes et al. 2007; Rinne et al. 2007, 2012). Strong et al. (2004) showed distributions of residence times, with the median varying from 20 s to 40 min depending on release height and leaf area distribution (full foliage versus defoliated forests). They concluded, especially for releases deeper into the forest, that there was ample time for chemical reactions to occur. Rinne et al. (2007, 2012) used a very similar LSM with very simple chemical reactions to estimate export fractions from two source heights for different canopies and different atmospheric conditions, also highlighting the importance of the in-canopy reactions in the interpretation of fluxes observed above the canopy for highly reactive BVOCs.

More recently, Bailey et al. (2014) used large-eddy simulation (LES) to estimate residence times in a non-homogeneous canopy (organized in row structures). They presented mean residence times as a function of *LAI* and concluded that residence times for particles released near the canopy top were not significantly affected by changes in *LAI* while differences were more significant for particles released in the lower canopy. They also observed an approximately linear increase in mean residence times with *LAI*, and proposed empirical fits with coefficients varying as a function of release location.

Although the Lagrangian framework is preferred in the definition of residence time, the export fraction can be estimated from Eulerian statistics as well. Edburg et al. (2012) used LES with passive scalar concentration fields and estimated the residence time using a canopy resistance analogy, showing a dependence of the bulk residence time on the vertical distribution of the scalar source. Despite this recent progress using LES, a simple theoretical model for estimating residence times is still not available.

In the present study, we develop a new theoretical framework to model the probability distribution function of residence times of air parcels released inside a forest canopy. The starting point of the theory is the Lagrangian framework adopted by Taylor (1922) to study diffusion in a field of homogeneous turbulence, complemented by the solution of the first-passage problem first derived by Schrödinger (1915) and a simple model of the eddy diffusivity within plant canopies. The model includes a simple treatment for first-order chemical reactions, comparable to previous work in the field (Strong et al. 2004; Fuentes et al. 2007; Rinne et al. 2012), to provide estimates of canopy export fractions of plant-emitted hydrocarbons. The framework is used to obtain two model solutions (with different levels of detail) that can be used to parametrize export fractions in regional and global atmospheric numerical models that do not resolve turbulent transport within plant canopies. Theoretical predictions for the residence times compare favourably with those obtained from LES for a range of canopy structures (including variations in LAI and vertical leaf area distribution) and turbulence levels under neutral stratification. Model predictions of export fraction as a function of the Damköhler number differ from those obtained from the empirical parametrization developed for the MEGAN model (Guenther et al. 2006, 2012).

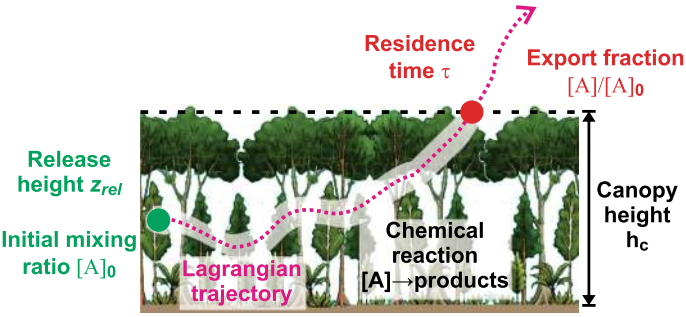

Fig. 1 Illustration of an air-parcel trajectory within a tall forest canopy

2 Theory

2.1 Definition of the Problem and Modelling Strategy

An idealized model scenario, including a very simple chemical reaction model, is employed here to study the in-canopy residence time of air parcels and their importance for within-canopy chemistry. Consider an air parcel with an initial gas mixing ratio $[A]_0$ of a generic chemical species, emitted at a height z_{rel} in a forest with canopy height h_c as illustrated in Fig. 1. The air parcel will follow a trajectory and eventually leave the forest after a residence time τ within the canopy. During its journey within the canopy, the gas mixing ratio will be modified by chemical reactions and by turbulent mixing between the air parcel and its surrounding environment. Here it is assumed that $[A]$ undergoes one or more reactions with a chemical lifetime τ_{chem}. Once it leaves the forest for the first time, the air parcel will contain a gas mixing ratio $[A]_\tau$, defining an associated export fraction $EF = [A]_\tau/[A]_0$. Distinct air parcels, even when released at the same height, will follow different trajectories, leading to a distribution of residence times and export fractions. Our main goal is to develop a theoretical model to predict the probability distribution function (PDF) of residence times for the air parcels for a given canopy configuration under defined turbulence conditions. A secondary goal is to assess the importance of the characteristics of the PDF on the chemical loss of $[A]$ and estimate its export fraction.

2.2 Model for Air-Parcel Residence Time Within Forests

A simple treatment of turbulent transport is required if an analytical model for residence time is to be developed. As frequently done in the development of theoretical models for canopy turbulence (e.g., Katul et al. 2004), turbulent transport is represented by an eddy diffusivity $K(z)$. The assumption that turbulent transport within plant canopies can be modelled via eddy diffusivity has been challenged in the literature (Denmead and Bradley 1985; Kaimal and Finnigan 1994). Here the eddy-diffusivity model is employed and its applicability in the present problem stands or falls based on the comparisons of theoretical model predictions with LES results (which do not rely on this assumption). These comparisons are presented in Sect. 4.4.

If the turbulent transport of air parcels is assumed to be diffusive with a constant eddy diffusivity, K_{eq}, then the time evolution of the PDF of the air-parcel position satisfies a simplified Fokker–Planck equation (Thomson 1987; Rodean 1996). See Appendix 1 for

details. In this context, the PDF of residence times is given by the distribution of first-passage through a plane at height $z = h_c$ (i.e., at a distance $|h_c - z_{\mathrm{rel}}|$ from the release height). For a diffusive process with constant eddy diffusivity, this first-passage distribution is given by (Cox and Miller 1965; Redner 2001—see "Appendix 1" for more details)

$$p(\tau; z_{\mathrm{rel}}) = \frac{|h_c - z_{\mathrm{rel}}|}{\sqrt{4\pi K_{\mathrm{eq}}}} \tau^{-3/2} \exp\left[-\frac{(h_c - z_{\mathrm{rel}})^2}{4K_{\mathrm{eq}}\tau}\right]. \tag{1}$$

Equation 1 is a simplified form of the inverse-Gaussian or Wald distribution for the special case of zero mean drift and it was first derived by Schrödinger (1915). In the context of turbulent dispersion within forests, Katul et al. (2005) used a similar approach to model the long distance dispersion of seeds with small settling velocity.

Note that Eq. 1 is a model for the PDF of air parcels originating at one specific release height inside the canopy. Therefore, this solution allows for the use of different effective eddy diffusivities for air parcels originating from different release heights. To include in the model as much of the vertical variation of $K(z)$ as possible, we introduce an equivalent eddy diffusivity $K_{\mathrm{eq}}(z_{\mathrm{rel}})$ as a representative value between release height and canopy height. Thus, for Eq. 1 to be applicable, the eddy diffusivity must be a constant for a given release height, but it can be different for different release heights.

For now we assume that Eq. 1 is a reasonable model and explore some of its implications. Note that the model predicts an exponential increase in probability followed by a fat-tailed $\tau^{-3/2}$ power-law decrease, suggesting the existence of a clear mode in the distribution. In addition, a turbulent transport time scale

$$\tau_{\mathrm{turb}}(z_{\mathrm{rel}}) = \frac{(h_c - z_{\mathrm{rel}})^2}{4K_{\mathrm{eq}}(z_{\mathrm{rel}})} \tag{2}$$

can be defined based on Eq. 1. The median residence time $\tau_{\mathrm{m}}(z_{\mathrm{rel}})$ can be determined from the PDF (Eq. 1) as the time for which the cumulative distribution function is equal to 1/2. Thus

$$\int_{-\infty}^{\tau_{\mathrm{m}}(z_{\mathrm{rel}})} p(\tau; z_{\mathrm{rel}})\mathrm{d}\tau = \mathrm{erf}\left(\frac{h_c - z_{\mathrm{rel}}}{\sqrt{4K_{\mathrm{eq}}(z_{\mathrm{rel}})\tau_{\mathrm{m}}}}\right) = \frac{1}{2}, \tag{3}$$

where erf is the error function. Noting that $\mathrm{erf}(a) = -1/2$ when $a \approx -0.477$ yields an explicit equation for the median residence time given by

$$\tau_{\mathrm{m}}(z_{\mathrm{rel}}) = \frac{1}{4a^2}\frac{(h_c - z_{\mathrm{rel}})^2}{K_{\mathrm{eq}}(z_{\mathrm{rel}})} \approx 1.10\frac{(h_c - z_{\mathrm{rel}})^2}{K_{\mathrm{eq}}(z_{\mathrm{rel}})}. \tag{4}$$

Finally, with the goal of developing simple bulk models that do not require detailed information on the canopy structure, one can also determine a canopy-integrated PDF of residence times by assuming that air parcels are released uniformly at all heights inside the canopy. However, the integration with respect to z_{rel} requires the additional assumption that the eddy diffusivity be constant for the entire canopy so that K_{eq} is not a function of z_{rel}. Even though this is not a very good assumption, it is necessary if an explicit analytical result is to be developed. Therefore, we replace $K_{\mathrm{eq}}(z_{\mathrm{rel}}) = K_{\mathrm{const}}$ to obtain

$$p_{h_c}(\tau) = \frac{1}{h_c}\int_0^{h_c} p(\tau; z_{\mathrm{rel}})\mathrm{d}z_{\mathrm{rel}} = \sqrt{\frac{K_{\mathrm{const}}}{\pi h_c^2}}\tau^{-1/2}\left[1 - \exp\left(\frac{-h_c^2}{4K_{\mathrm{const}}\tau}\right)\right]. \tag{5}$$

It is useful to verify the behaviour of this canopy-integrated PDF in the limit of very large τ. For $\tau \gg h_c^2/(4K_{\mathrm{const}})$, the exponential term in Eq. 5 can be approxi-

mated as $\exp\left(-h_c^2/(4K_{\text{const}}\tau)\right) \approx \left[1 - h_c^2/(4K_{\text{const}}\tau)\right]$ and the solution becomes $p_{h_c}(\tau) \approx \left[h_c/\left(4\sqrt{K_{\text{const}}\pi}\right)\right]\tau^{-3/2}$, indicating that the canopy-integrated PDF also displays the $\tau^{-3/2}$ power-law decay for large residence times.

To completely specify the solution, a model for the eddy diffusivity $K(z)$ within the canopy is required. We use the expression $K(z) = \sigma_w^2(z)T_L(z)$ derived for the far-field diffusion regime by Taylor (1922), where σ_w^2 is the vertical velocity variance and T_L is the Lagrangian integral time scale. Following Raupach (1989), we adopt a constant integral time scale inside the canopy given by $T_L/(h_c/u_*) = 1/3$. For the vertical velocity variance, we adopt a simple model suggested by LES results presented in Sect. 4 and given by

$$\frac{\sigma_w}{u_*} = c_1\left[\frac{\exp(c_2 z/h_c) - 1}{\exp(c_2) - 1}\right], \tag{6}$$

where c_1 is a constant that sets the value of σ_w/u_* at the canopy top and $c_2(LAI)$ sets the curvature of the profile depending on the total leaf area index [the shape of this profile is not too different from the more complex model proposed by Massman and Weil (1999)]. These two coefficients are determined using LES results in Sect. 4. The resulting eddy-diffusivity model is given by

$$K(z) = \frac{c_1^2}{3}\left[\frac{\exp(c_2 z/h_c) - 1}{\exp(c_2) - 1}\right]^2 u_* h_c, \tag{7}$$

and to complete the canopy-resolved model given by Eq. 1 and the bulk model given by Eq. 5, the relation between the vertically varying eddy diffusivity Eq. 7 and the equivalent eddy diffusivities $K_{\text{eq}}(z_{\text{rel}})$ and K_{const} must be specified. In the case of $K_{\text{eq}}(z_{\text{rel}})$, Freire et al. (2017) argued that a simple average of $K(z)$ between z_{rel} and h provides an upper bound of the true diffusivity, while a resistance model (i.e., an average of the reciprocal of the diffusivity) provides a lower bound. Here, we use a geometric mean, which yields values in between the two other models, to estimate $K_{\text{eq}}(z_{\text{rel}})$. The generalization of the geometric mean for a continuous function is given by the product integral (Dannon 2011)

$$K_{\text{eq}}(z_{\text{rel}}) = \left(\prod_{z=z_{\text{rel}}}^{z=h_c} K(z)^{\mathrm{d}z}\right)^{1/(h_c - z_{\text{rel}})} = \exp\left(\frac{\int_{z_{\text{rel}}}^{h_c} \ln\left(K(z)\right)\mathrm{d}z}{(h_c - z_{\text{rel}})}\right). \tag{8}$$

For the constant eddy diffusivity required in the bulk model (Eq. 5), we use an arithmetic mean mostly because the main advantage of the bulk model is to obtain an explicit expression that can be used for parametrization in regional and global models. As will be shown later, this simplification does not compromise the accuracy of the model. Thus, we write

$$K_{\text{const}} = \frac{1}{h_c}\int_0^{h_c} K(z)\mathrm{d}z = \frac{1}{3}g(LAI)u_* h_c, \tag{9}$$

where

$$g(LAI) = c_1^2\frac{(2c_2 - 4\exp(c_2) + \exp(2c_2) + 3)}{2c_2\left(\exp(c_2) - 1\right)^2}. \tag{10}$$

One can certainly improve the representation of the eddy diffusivity by selecting more complex models for $K(z)$ (e.g. Massman and Weil 1999; Katul et al. 2004), but as will be shown in Sect. 4, the simple model selected here provides good estimates for the quantities of interest.

2.3 Model for the Export Fraction of Reacting Scalars

For the sake of analytical tractability, it is assumed here that the loss of $[A]$ is due only to chemical reactions in the forest, and mixing between the air parcel and the environment is neglected. In addition, a pseudo first-order approximation will be used to represent the loss of $[A]$ during the air-parcel trajectory inside the canopy, which is given by

$$\frac{\mathrm{d}[A]}{\mathrm{d}t} = -\frac{1}{\tau_{\mathrm{chem}}}[A], \tag{11}$$

where τ_{chem} is the chemical lifetime of $[A]$ representing the combined result of all the relevant chemical reactions. By further assuming τ_{chem} to be a constant, the solution is

$$[A](t) = [A]_0 \exp\left(-t/\tau_{\mathrm{chem}}\right), \tag{12}$$

providing an explicit relationship between residence time τ and the export fraction given by $EF = \exp\left(-\tau/\tau_{\mathrm{chem}}\right)$.

By combining the theoretical model for the distribution of residence times obtained from the first-passage method (Eq. 1) with the pseudo first-order chemical reaction it is possible to formulate a mathematical model for the fraction of $[A]$ leaving the canopy within a period of time t after the gas release. By definition, the export fraction during the period t, denoted $EF_t(t; z_{\mathrm{rel}})$, is given by

$$EF_t(t; z_{\mathrm{rel}}) = \int_0^t p(\tau; z_{\mathrm{rel}}) \exp\left(-\tau/\tau_{\mathrm{chem}}\right) \mathrm{d}\tau, \tag{13}$$

and using Eq. 1, the integral above can be evaluated, with the result

$$\begin{aligned} EF_t(t; z_{\mathrm{rel}}) = & \frac{1}{2} \exp\left(-2\sqrt{\frac{\tau_{\mathrm{turb}}}{\tau_{\mathrm{chem}}}}\right) \left\{1 - \mathrm{erf}\left(\sqrt{\frac{\tau_{\mathrm{turb}}}{t}} - \sqrt{\frac{t}{\tau_{\mathrm{chem}}}}\right)\right. \\ & \left. - \exp\left(4\sqrt{\frac{\tau_{\mathrm{turb}}}{\tau_{\mathrm{chem}}}}\right) \left[\mathrm{erf}\left(\sqrt{\frac{\tau_{\mathrm{turb}}}{t}} + \sqrt{\frac{t}{\tau_{\mathrm{chem}}}}\right) - 1\right]\right\}. \end{aligned} \tag{14}$$

Equation 14 reveals the interplay between three relevant time scales involved in this problem: the time since release (t), the chemical time scale τ_{chem}, and the turbulent transport time scale τ_{turb}. In the limit when $t \to \infty$, the equation simplifies to

$$EF_\infty(z_{\mathrm{rel}}) = \exp\left(-2\sqrt{\frac{\tau_{\mathrm{turb}}}{\tau_{\mathrm{chem}}}}\right) = \exp\left[-2\left(\frac{(h_c - z_{\mathrm{rel}})^2}{4K_{\mathrm{eq}}(z_{\mathrm{rel}})\tau_{\mathrm{chem}}}\right)^{1/2}\right], \tag{15}$$

allowing estimation of the export fraction of $[A]$ for sources located at $z = z_{\mathrm{rel}}$. Note that this solution can be expressed as a function of a Damköhler number that depends on the release height z_{rel} as $EF_\infty(z_{\mathrm{rel}}) = \exp\left(-2\sqrt{Da(z_{\mathrm{rel}})}\right)$. However, it is more useful in practice to use a single Damköhler number defined based on conditions at the top of the canopy given by $\mathrm{Da} = (h_c/u_*)/\tau_{\mathrm{chem}}$. The solution above can then be recast in the form

$$EF_\infty(z_{\mathrm{rel}}) = \exp\left[-2\left(\frac{(1 - z_{\mathrm{rel}}/h_c)^2}{4K^*_{\mathrm{eq}}(z_{\mathrm{rel}})}Da\right)^{1/2}\right], \tag{16}$$

where $K^*_{\mathrm{eq}}(z_{\mathrm{rel}})$ is the normalized eddy diffusivity given by $K^*_{\mathrm{eq}}(z_{\mathrm{rel}}) = K_{\mathrm{eq}}(z_{\mathrm{rel}})/(h_c u_*)$.

Finally, if the vertical distribution of the source of $[A]$, $q_{[A]}(z)$, within the forest is known, one can obtain the total export fraction EF_{tot} by integrating

$$EF_{\text{tot}} = \int_0^{h_c} q_{[A]}(z_{\text{rel}}) EF_{\infty}(z_{\text{rel}}) \mathrm{d}z_{\text{rel}}. \tag{17}$$

Equations 16 and 17 can be integrated numerically with any gas source profile to yield an estimate of the total gas export fraction. As discussed in the previous sub-section, this model relies on a representative constant $\tau_{\text{turb}}(z_{\text{rel}})$ (or $K_{\text{eq}}(z_{\text{rel}})$) for each layer. Similarly, if τ_{chem} presents significant variation in the vertical direction, a representative constant chemical time scale can be defined for each layer $\tau_{\text{chem}}(z_{\text{rel}})$. Therefore, this model accounts in a simplified way for vertical variations in canopy morphology, emissions of $[A]$ and chemical lifetime of $[A]$. The use of this model requires the following information: (1) vertical distribution of the source of $[A]$, (2) vertical distribution of oxidant levels inside the canopy to determine τ_{chem} at each level, and (3) vertical profiles of eddy diffusivity $K(z)$ to determine τ_{turb}. The latter can be obtained from values of u_* and information of canopy structure (canopy height and LAI) using Eq. 7.

An explicit solution to Eq. 17 can be obtained if the source $q_{[A]}(z)$ and the eddy diffusivity $K(z)$ are assumed to be independent of height. Because the emission of many BVOCs is temperature as well as light dependent and takes place mostly near the canopy top, a constant emission is assumed between a generic height $z = \alpha h_c$ and the canopy top. Thus, a uniform source with strength $q_{[A]}(z) = 1/[(1-\alpha)\, h_c]$ is assumed, and the integration of Eq. 17 between an arbitrary level αh_c and h_c yields

$$EF_{\text{tot}} = \left(\frac{K^*_{\text{const}}}{(1-\alpha)^2 Da} \right)^{1/2} \left\{ 1 - \exp\left[- \left(\frac{(1-\alpha)^2 Da}{K^*_{\text{const}}} \right)^{1/2} \right] \right\}, \tag{18}$$

where $K^*_{\text{const}} = K_{\text{const}}/(h_c u_*)$. Equation 18 is a simplified version of the model given by Eqs. 16 and 17, and only requires information on the concentration of τ_{chem} within the forest, u_*, and h_c and LAI. The parameter α can be used to adjust the emission profile of $[A]$ by, for example, excluding a trunk space, which may not contribute to emissions. As will be discussed later, in the case of $\alpha > 0$, it may be more appropriate to use a modified K_{const} defined as the average of $K(z)$ over the range where the emissions occur, which yields

$$K_{\text{const},\alpha} = \frac{1}{3} G(LAI; \alpha) u_* h_c, \tag{19}$$

where

$$G(LAI; \alpha) = c_1^2 \frac{\left[2c_2(1-\alpha) + (\exp(c_2) - \exp(\alpha c_2))(\exp(c_2) + \exp(\alpha c_2) - 4) \right]}{2c_2(1-\alpha)\,(\exp(c_2) - 1)^2}. \tag{20}$$

As expected, $G(LAI; \alpha = 0) = g(LAI)$ given by Eq. 10.

It is important to emphasize that in the present model, $K(z)$, $K_{\text{eq}}(z_{\text{rel}})$, and K_{const} are all eddy diffusivities for fluid parcels, as in the original modelling framework used by Taylor (1922). Note that in many instances, in particular when simple solutions based on the Reynolds-averaged Navier–Stokes equations are sought, the chemical reactions are lumped in to the eddy-diffusivity model adopted to close the turbulent flux term (e.g., see Hamba 1993). This approach requires the introduction of a modified eddy diffusivity that is a function of the Damköhler number. LES results presented by Patton et al. (2001) confirm that the eddy diffusivity does depend on Da. Nevertheless, in the present approach the two processes are treated separately in the sense that the Lagrangian particles are transported by turbulence

and the loss of the reacting gas due to chemistry is represented by the simple decay model (Eq. 12). Thus, no modifications of the eddy diffusivity are needed.

2.4 Model Applicability to Estimate Oxidation of BVOCs

The application of the theoretical model to estimate the oxidation of BVOCs within forest canopies requires a number of assumptions, but it is a useful exercise in the sense that it can provide more physical insight into parametrizations that are, to date, completely empirical. For the case of the rainforest, the dominant oxidants that react with BVOCs include ozone (O_3), the hydroxyl radical (OH), and the nitrate radical (NO_3), so that the total reactivity could be approximated by $\sum k_{\chi_i}[\chi_i] = k_{O_3}[O_3] + k_{OH}[OH] + k_{NO_3}[NO_3]$, where k_{χ_i} and $[\chi_i]$ are the reaction rate constants and concentrations for a number of generic oxidants χ_i. If these reactions are modelled following the pseudo first-order approach as done in many previous studies (Strong et al. 2004; Fuentes et al. 2007; Jardine et al. 2011; Rinne et al. 2012), the model presented in the previous sub-section is still applicable if the chemical time scale is now defined as $\tau_{chem} = \tau_{oxi} = 1/\sum k_{\chi_i}[\chi_i]$ (and consequently $Da = (h_c/u_*)/\tau_{oxi}$).

The most accurate version of the theoretical model requires the numerical integration of Eqs. 16 and 17, while the simplest model is given by Eq. 18 with the modified $K^*_{const,\alpha} = G(LAI;\alpha)/3$. For the latter, τ_{oxi} has to be constant and must be defined based on representative mean values of the levels of the three oxidants. This equation can be compared to the empirical parametrization of in-canopy chemical loss developed for the MEGAN model (Guenther et al. 2006), which is given by

$$EF_{tot} = 1 - \frac{\beta h_c}{\lambda u_* \tau_{megan} + \beta h_c} = \frac{1}{1 + (\beta Da)/\lambda}, \tag{21}$$

where τ_{megan} is the lifetime of the BVOC above the canopy, β is the fraction of the canopy occupied by leaves (i.e. to exclude trunk space), and $\lambda = 0.3$ is an empirical constant (βh_c is used here in place of D as in the original formulation to highlight the similarities between the two models). Note that τ_{megan} is equivalent to τ_{oxi} and the same information is present in both models (except for the explicit inclusion of LAI in Eq. 18). These models are compared in Sect. 4.

3 Large-Eddy Simulations

Given the assumptions about turbulent transport required in the development of the theoretical model for the PDF of residence times inside the canopy, an assessment of its applicability is required. However, due to the Lagrangian nature of the problem, residence times cannot be easily obtained from typical Eulerian-based experimental datasets. Therefore, one needs to rely on LES as the standard against which simple analytical models can be assessed. The approach adopted here consists in first assessing the accuracy of the LES by comparing its results with observational data from the Amazon rainforest and then using the LES to assess the theoretical model. This is accomplished by using the LES turbulent velocity field to drive a Lagrangian particle tracking model, which in turn allows direct calculation of the PDF of residence times as a function of release height.

3.1 Observational Dataset for Model Assessment

The numerical simulations presented are based on turbulence data obtained during a field campaign that was conducted from March 2014 to January 2015 at the Cuieiras Biological Reserve (2°36′32″S, 60°12′ 33″W), located approximately 60 km north-north-west of the city of Manaus, Brazil (Fuentes et al. 2016). The vegetation of the site is a dense primary forest with canopy height between 30 and 40 m, with the area characterized by a sequence of valleys and plateaus with altitude differences of about 60 m. While soils of the valleys are sandy and the vegetation is shorter and less dense, loamy soils on the plateaus support denser and taller vegetation. The LAI values on the plateaus are estimated to be between 5.7 and 7.3 $m^2 m^{-2}$ (McWilliam et al. 1993; Marques Filho et al. 2005; Tóta et al. 2012). Hereafter we adopt $h_c = 35$ m with $LAI = 6$ and a leaf area density profile reported by Tóta et al. (2012) (Fig. 2a). On one of the plateaus, the 50-m high K34 tower was instrumented with a vertical array of nine triaxial sonic anemometers (model CSAT-3, Campbell Scientific Inc., Logan, Utah) to study turbulent motions within and above the canopy. Sonic anemometer heights corresponded to $z\,h_c^{-1} = 0.20$, 0.39, 0.52, 0.63, 0.70 ,0.90, 1.00, 1.15, and 1.38. The three components of wind velocity (u, v, w) were recorded at a frequency of 20 Hz. Additionally, a separate sonic anemometer was placed at 1.5 m above the ground ($z\,h_c^{-1} = 0.043$) in the vicinity of the tower, and all sonic measurements were corrected for transducer shadowing following Horst et al. (2015).

For comparison with LES results, turbulence statistics were calculated for stationary periods under near-neutral conditions. Stationarity was determined following Foken et al. (2004) using a criterion of 50% deviation on kinematic momentum fluxes. The criterion $-0.03 < h_c/L < 0.06$ was used to characterize near-neutral conditions ($L = -u_*^3 \overline{T}_v/(\kappa g \overline{w'T_v'}|_{h_c})$ is the Obukhov length scale). This interval is three times as large as that proposed by Dupont and Patton (2012) to ensure that a sufficiently large number of 30-min periods (ranging from 163 at $z/h_c = 0.52$ to 506 at $z/h_c = 1.00$) per level were available. The friction velocity, u_*, was defined based on the kinematic momentum flux for the rotated wind vector at the canopy height ($u_* = \sqrt{-\overline{u'w'}|_{h_c}}$), $\overline{T}_v$ is the mean virtual air temperature at the canopy height, $\kappa = 0.4$ is the von Karman constant, g is the acceleration due to gravity, and $\overline{w'T_v'}|_{h_c}$ is the kinematic virtual heat flux also defined at canopy height. Furthermore, only data for flow directions (u_{dir}) in the range $-90° < u_{\mathrm{dir}} < 90°$ relative to the sensor head were used (in order to minimize the influence of flow distortion due to the tower and the sonic anemometer's body).

3.2 Numerical Simulations

Chamecki et al. (2008, 2009) and Pan et al. (2014a) describe the LES model used in this study. It uses a pseudo-spectral discretization in the horizontal directions and a second-order centered finite difference discretization in the vertical direction. Non-linear terms are fully dealiased using the 3/2 rule by padding and increasing the size of the vectors when calculating products (Canuto et al. 2012). As in all LES approaches, the velocity vector ($\mathbf{u}$) is split into a resolved part (i.e., $\tilde{\mathbf{u}}$) and subgrid-scale contribution for scales smaller than a characteristic grid scale Δ. The subgrid-scale stress tensor is calculated according to a Smagorinsky model using the scale-dependent Lagrangian averaged dynamic approach (Bou-Zeid et al. 2005). The simulation domain is periodic in both horizontal directions and flat topography is assumed. At the top boundary, no-stress and no-penetration boundary conditions are enforced, and for the bottom boundary condition, a wall model based on the

logarithmic law is used. The LES resolves the canopy in the sense that for levels within the forest a drag force representing the effects of vegetation is applied to every grid cell following Shaw and Schumann (1992). The drag force, $\mathbf{d}$, exerted by the forest canopy on the airflow is parametrized as

$$\mathbf{d} = -C_d \left(\mathbf{P}a(z)\right) \cdot \left(|\tilde{\mathbf{u}}|\tilde{\mathbf{u}}\right), \tag{22}$$

where C_d is a constant drag coefficient and $a(z)$ is the leaf area density. $\mathbf{P}$ is a diagonal tensor that projects the total leaf area density into planes perpendicular to each of the three spatial dimensions (Pan et al. 2014a). In the absence of direct measurements, we assume a uniform random distribution for leaf orientation, which results in $P_x = P_y = P_z = 1/2$ (for a sphere, which has uniformly distributed surface normals, the projected area onto any given plane is 1/2 of the total surface area). The leaf area density is assumed to be horizontally homogeneous, and spatial patterns in the forest structure are not represented in the model.

The determination of residence times requires tracking of air-parcel trajectories, which are obtained by integrating (Weil et al. 2004)

$$\frac{d\mathbf{x}_{\mathrm{p,i}}}{\mathrm{d}t} = \tilde{\mathbf{u}}_{\mathrm{i}} + \mathbf{u}_{\mathrm{sgs,i}}, \tag{23}$$

where $\mathbf{x}_{\mathrm{p,i}}$ is the position of the ith air parcel. Here, $\tilde{\mathbf{u}}_{\mathrm{i}}$ is the resolved velocity at the particle location, obtained by linear interpolation of the LES-resolved velocity in the three spatial directions. The subgrid-scale velocity at the air-parcel location $\mathbf{u}_{\mathrm{sgs,i}}$ is modelled using the Langevin equation as described in Weil et al. (2004), but using the modifications for compatibility with the Lagrangian-averaged subgrid-scale model introduced by Bailey et al. (2014).

The horizontal periodicity of the domain is extended to the Lagrangian tracking, in the sense that particles travelling across a horizontal boundary are recirculated. The Lagrangian model does not account for deposition of air parcels and the lower surface is assumed to be fully reflective (with elastic collisions). To determine in-canopy air residence times (τ), each air parcel is tracked until it leaves the canopy and is given a unique τ corresponding to the time between the release of the air parcel and the first time when the height of the parcel exceeds h_{c}. Subsequent movements across the canopy top, which occasionally occur, are not taken into account.

3.3 Simulation Set-Up

The simulation domain represents a box with dimensions $L_x \times L_y \times L_z$ equal to $32\,h_{\mathrm{c}} \times 21.33\,h_{\mathrm{c}} \times 10.66\,h_{\mathrm{c}}$, discretized using $144 \times 96 \times 192$ grid points, respectively, and corresponding to a grid resolution of $8\,\mathrm{m} \times 8\,\mathrm{m} \times 2\,\mathrm{m}$. The horizontal model domain and the first 18 vertical layers are occupied by horizontally homogeneous distribution of vegetation (this effectively sets $h_c = 36\,\mathrm{m}$ in the LES instead of $h_c = 35\,\mathrm{m}$ considered in the measurements). The vertical domain of approximately $10\,h_{\mathrm{c}}$ is expected to be sufficient for the LES to resolve the dominant scales of motion that occur in the region of interest $z/h_c \leq 2$ (Bailey and Stoll 2013; Pan et al. 2014a; Pan and Chamecki 2016). Note that the integral length scales for the horizontal and vertical velocity components in simulations that resolve the entire neutral atmospheric boundary layer (ABL) are smaller than $2h_c$ for $z/h_c \leq 2$ (Patton et al. 2016). For the roughness length (z_0) of the lower boundary wall model, we take $z_0 = 0.01\,\mathrm{m}$. In all simulations, the velocity field evolves for 1.25 h allowing the turbulence to reach a statistically stationary state. Turbulence statistics are then calculated for the subsequent 1.25 h and the LES is run for an additional 0.5 h for the integration of the Lagrangian model. The LES timestep $\Delta t = 0.01\,\mathrm{s}$ to ensure that the Courant-Friedrichs-Lewy condition (e.g., see

Peyret and Taylor 2012) is satisfied to ensure stability of the explicit time integration scheme throughout the simulation.

The canopy drag coefficient ($C_d = 0.4$) was determined from the divergence of the vertical momentum flux estimated from measurements following Cescatti and Marcolla (2004). Data for $z\,h_c^{-1} < 0.7$ were not used because the divergence of the momentum flux is small in the bottom canopy and the drag force is mostly balanced by mean pressure gradients that were not measured. The value of C_d yields an effective drag coefficient $C_d P_x = 0.2$, which is in good agreement with the frequently used range of $C_d P_x = 0.1$–0.4 for forests (Queck et al. 2011).

Buoyancy effects are not considered in the LES, as they are not the focus of the study, and due to the limited spatial scale of the simulation, the Coriolis force is considered negligible. Ten LES runs were performed to study the effects of canopy structure, total LAI, and u_* on air-parcel residence times. The timestep (δt) of the Lagrangian model was set to $\delta t = 10\Delta t = 0.1$ s, as a compromise between accuracy, computational costs and storage needs. Based on typical vertical velocities in the order of 0.1–1 m s^{-1} and the vertical resolution of 2 m, such a timestep appears sufficient to avoid rogue trajectories arising from the numerical instability of the subgrid-scale velocity calculation (Yee and Wilson 2007) and it is more restrictive than the criterion $\delta t = 0.04h/u_*$ used by Bailey et al. (2014). The transport of air parcels (Eq. 23) was numerically integrated with the explicit second-order Adams–Bashfort scheme, while the subgrid-scale velocity portion was updated using a combination of implicit and Euler forward time-stepping (Bailey et al. 2014). Lagrangian particles were released during the first 2000 timesteps (20 s) of the 30-min simulation. During each of those timesteps 1000 particles were released at 10 heights that were spaced at regular intervals between $z_{\mathrm{rel}} = 0.1\,h_{\mathrm{c}}$ and $1\,h_{\mathrm{c}}$, yielding a total of 2×10^6 particles per release level. Particles were released from the central 1000 m × 480 m of the domain (spaced 20 and 24 m apart in x- and y-directions). The PDF of air-parcel residence times converged well below the 2×10^6 particles released per level (data not shown).

The control simulation (CTL) was designed to approximate the canopy structure of the field site. The leaf area distribution from Tóta et al. (2012), shown in Fig. 2a, is normalized to a total $LAI = 6\,\mathrm{m}^2\,\mathrm{m}^{-2}$, which corresponds approximately to the value of Marques Filho et al. (2005). This choice was made because the former was collected from an airborne sensor with high vertical resolution over a larger area, while the latter was measured at the location of the tower. The flow in the LES was driven by an imposed mean pressure gradient force, which in steady-state conditions is balanced by a shear stress at the surface defining a unique value for the friction velocity. We used $u_* = 0.4\,\mathrm{m\,s^{-1}}$ as a representative value of daytime conditions based on the daytime median $u_* = 0.41\,\mathrm{m\,s^{-1}}$ obtained from the observational dataset. The results of this simulation are compared to field data in Sect. 4.

Additional simulations were performed to assess the sensitivity of the agreement between theoretical model and LES to canopy structures and turbulence conditions (Table 1). The effects of turbulence levels are determined by selecting $u_* = 0.1$ and $0.8\,\mathrm{m\,s^{-1}}$ (cases u_*1 and u_*8) for low and high turbulence cases. The lower value corresponds to typical early morning or nighttime (≈40th percentile) conditions, while $u_* = 0.8\,\mathrm{m\,s^{-1}}$ is an extreme value (97.5th percentile of daytime values) observed mainly during storms. Three idealized canopies were chosen by specifying leaf-area-density profiles using β-distributions to investigate the effects of canopy structure on residence times (see Fig. 2a). The first case ($\beta13$) has its maximum leaf area density at $(1/3)h_c$ while the second case ($\beta23$) has its maximum leaf area density at $(2/3)h_c$. For both cases, the shape parameter of the β-function was chosen so that the maximum normalized LAI matched the profile of Tóta et al. (2012). The third idealized leaf area distribution is a bimodal combination (Bim) of the two previous cases, having a greater

Table 1 Leaf area indices (LAI) and friction velocity values considered in the numerical simulations

Case	Leaf area distribution	LAI ($m^2\ m^{-2}$)	u_* ($m\ s^{-1}$)
CTL	Tóta et al. (2012)	6	0.4
$\beta 13$	β-distr. with $LAI_{max} = 1/3h_c$	6	0.4
$\beta 23$	β-distr. with $LAI_{max} = 2/3h_c$	6	0.4
Bim	combination of β 13 and $\beta 23$	6	0.4
L30	Tóta et al. (2012)	3	0.4
L45	Tóta et al. (2012)	4.5	0.4
L75	Tóta et al. (2012)	7.5	0.4
L90	Tóta et al. (2012)	9	0.4
u_*1	Tóta et al. (2012)	6	0.1
u_*8	Tóta et al. (2012)	6	0.8

leaf area distribution at the canopy top, with the $\beta 13$ case reduced by 20 %. Subsequently, the whole distribution was normalized to yield a total $LAI = 6\,m^2\,m^{-2}$. An additional set of simulations (L30–L90) investigates the importance of canopy density by varying LAI from 3 to 9.

4 Results and Discussion

4.1 LES Results

There is reasonable overall agreement between turbulence statistics from LES and from measurements made at the K34 forest (Fig. 2). Simulated wind speeds in the upper canopy region are higher than the observed values, likely due to uncertainties in the leaf area density (which is quite low in the uppermost third of the canopy). For the vertical momentum flux, agreement between LES and observations is good. A high percentage of the vertical momentum flux is due to resolved motions, as indicated by the proximity of the dashed and solid lines in Fig. 2c (all other statistics are calculated using only the resolved velocity field). The good agreement for standard deviations of horizontal and vertical velocity fluctuations illustrates that LES reliably reproduces turbulence conditions within the canopy. Despite the fact that the LES underestimates the standard deviations above the forest, the overall agreement is very good. Note that most LES of neutral canopy flows tend to yield $\sigma_w/u_* \approx 1$ at the canopy top (e.g., Pan et al. 2014a; Patton et al. 2016), even though experimental data suggest values closer to 1.25 for near-neutral conditions (Finnigan 2000).

As discussed in detail by Pan et al. (2014a), good agreement between first- and second-order moments does not guarantee a good representation of higher-order moments or the momentum transport partition into sweeps ($w' < 0; u' > 0$) and ejections ($w' > 0; u' < 0$). Peak of skewness, Sk_u, and the ratio of momentum due to sweeps to momentum due to ejections $S_{4,0}/S_{2,0}$ are good indicators of the penetration depth of mixing-layer eddies in the upper canopy region (Pan et al. 2014b). Good agreement between LES results and observations is obtained for both Sk_u and $S_{4,0}/S_{2,0}$. Furthermore, both Sk_u and $S_{4,0}/S_{2,0}$ reach zero at heights similar to the estimated penetration depth of canopy mixing-layer eddies obtained from the shear length scale $\ell_S = (\partial\overline{u}/\partial z)|_h/\overline{u}(h)$ (the LES mean velocity

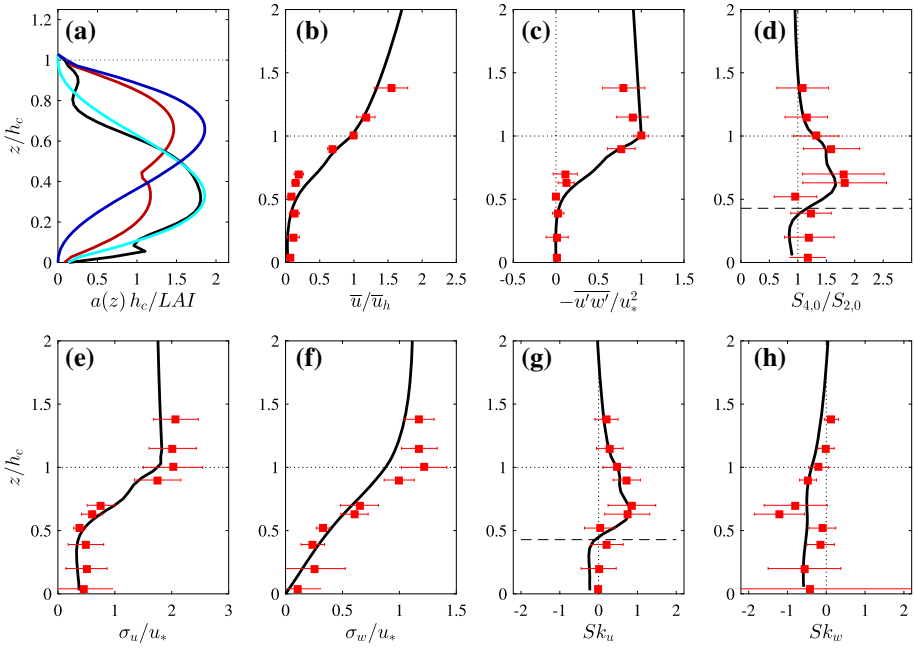

Fig. 2 Vertical profiles of leaf area density and turbulence statistics inside and above the forest. **a** vertical profiles for leaf area density used in the LES runs [CTL (*black*), β13 (*cyan*), β23 (*blue*), and Bim (*red*)]. LES results (*solid line*) and field observations (*red squares* for K34 data) are shown for **b** mean wind speed, **c** mean vertical momentum flux, **d** ratio of momentum due to sweeps to momentum due to ejections, standard deviations of **e** streamwise and **f** vertical velocity fluctuations, and skewness of **g** streamwise, and **h** vertical velocity. The *dashed line* in panel **c** represents the resolved momentum flux. *Horizontal dashed lines* in panels **d** and **g** mark the penetration depth of canopy mixing-layer eddies estimated by the shear length scale ℓ_S

profile yields $\ell_S/h_c \approx 0.52$ indicating that the eddies penetrate down to $z/h_c \approx 0.48$). It is not clear why Sk_u becomes negative in the lower canopy, but this effect is also present in the observations (even though the magnitude of negative Sk_u is much smaller in the observations and is consistent with the dominance of ejections over sweeps predicted by LES for this region of the canopy (Fig. 2d). Momentum fluxes in the lower canopy are very small in magnitude for both the LES and observations, making it difficult to determine reliable values for $S_{4,0}/S_{2,0}$. Finally, the skewness of vertical velocity Sk_w is also in reasonably good agreement with the observations. The LES misses the peak value at $z/h_c = 0.63$ and has a smoother variation with height in the lower canopy, though it is not clear why the observations have nearly zero Sk_w at $z/h_c = 0.2$ and 0.39. From this analysis, we conclude that there is overall good agreement between LES and observations, and the mixing-layer eddies do not penetrate below $z/h_c \approx 0.48$ as suggested by the shear length scale ℓ_S.

Turbulence statistics within the canopy depend on the characteristics of the forest structure. Figure 3 displays the sensitivity of turbulence profiles to variations in the leaf-area-density profile and total LAI. The main differences in turbulence properties are associated with "top heavy" and "non-top heavy" leaf-area-density distributions. The top heavy distributions reduce the penetration of mixing layer eddies, as illustrated by the ratios of momentum transported by sweeps and ejections (Fig. 3d). Increasing LAI reduces the penetration of mixing-layer eddies and reduces momentum fluxes and turbulent kinetic energy within the canopy (Fig. 3d). Interestingly ℓ_S provides a good estimate for the penetration of mixing-

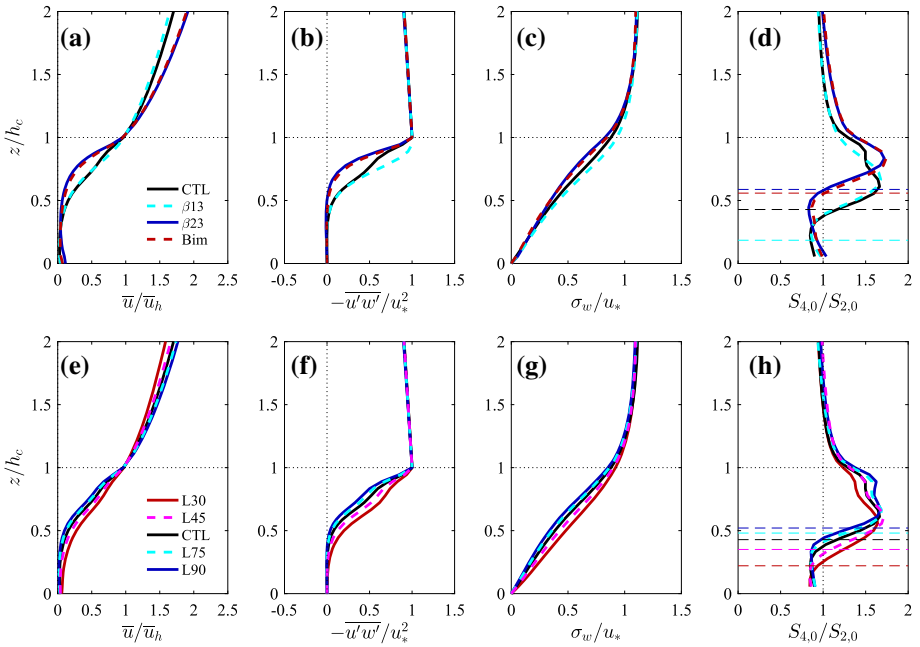

Fig. 3 Sensitivity of turbulence profiles to variations in leaf area density (**a**–**d**) and LAI (**e**–**h**). **a**, **e** Mean wind speed, **b**, **f** mean vertical momentum flux, **c**, **g** standard deviation of vertical velocity fluctuations, and **d**, **h** ratio of momentum of sweeps to momentum of ejections. See Table 1 for description of runs. *Horizontal dashed lines* in panels **d** and **h** mark the penetration depth of canopy mixing-layer eddies estimated by the shear length scale ℓ_S

Table 2 Fit of σ_w/u_* using Eq. 9 to values from LES for a constant $c_1 = 0.9$, and root-mean-square difference between fit and LES (*RSMD*)

	CTL	L30	L45	L75	L90	$\beta 13$	$\beta 23$	Bim	u_*1	u_*8
c_2	0.53	−0.36	0.12	0.78	1.01	0.14	1.02	1.22	0.47	0.54
RMSD	0.031	0.066	0.042	0.042	0.059	0.108	0.140	0.162	0.032	0.032

layer eddies for all cases except for β_{13}, for which it significantly overestimates the depth. Changes in neither the leaf area distribution nor the LAI are capable of reproducing the observed abrupt decreases in wind speeds and turbulence levels between $z/h_c = 0.7$ and 0.9 (Fig. 3).

Of particular relevance is the response of σ_w/u_* to changes in canopy structure, which is critical for vertical transport and needs to be parametrized in the theoretical model. To a good approximation, all the profiles in Fig. 3c,g collapse around $\sigma_w/u_* \approx 0.9$ at canopy top and go to zero (by definition) at the ground. These profiles motivate the model for σ_w/u_* given by Eq. 6. Thus, we set $c_1 = 0.9$ and fit $c_2(LAI)$ by minimizing the root mean square error to capture the effect of LAI in the curvature on the profiles (see Table 2 for values and quality of fit). Note that even though c_2 is a function only of LAI (and not the vertical canopy structure), different values are used for different leaf area density profiles.

The resulting $K(z)$ (Eq. 7) quickly decrease with height inside the canopy (Fig. 4). Changing the LAI from 3 to 9 causes a maximum reduction of $K(z)$ by approximately 50% at

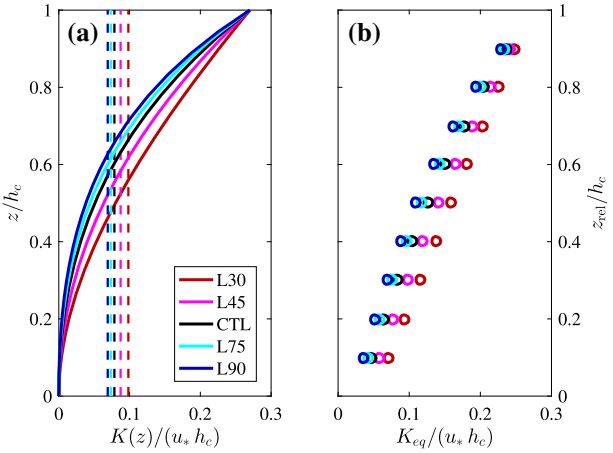

Fig. 4 Normalized modelled eddy-diffusivity profiles for cases with LAI varying from 3 to 9 for **a** $K(z)$ from Eq. 7 (*solid lines*) and bulk eddy diffusivity K_{const} from Eq. 9 (*dashed lines*) and **b** equivalent eddy diffusivity $K_{\text{eq}}(z_{\text{rel}})$ from Eq. 8

$z/h_c = 0.6$. In the lower third of the canopy values of $K(z)$ are small. The equivalent eddy diffusivity based on the product integral (Eq. 8) used in the theoretical model is shown for comparison in Fig. 4b. Resulting values are much smaller than the bulk eddy diffusivity K_{const} for release height near the bottom of the canopy, and tend to the local eddy diffusivity at the top of the canopy.

4.2 Air-Parcel Residence Times: The Amazon Rainforest Case

Median air-parcel residence times for the CTL simulation increase from less than 1 min for air parcels released at the canopy top to approximately 30 min for air parcels released deep inside the forest (Fig. 5a). Note that the simulation is 30-min long and that this time period is sufficient for determining the median residence time for all release heights in the CTL simulation, but not for all the particles to move out of the canopy (requiring a truncation for lower levels in Fig. 5a). From the distribution of residence times, it is immediately apparent that air-parcel residence times are skewed towards larger values and skewness increases in the lower canopy. As a consequence, statistical measures (such as the mean or median) are not enough to characterize the time that is available for reactive gases to undergo chemical reactions within the canopy. Given the large skewness of the distribution, maximum air-parcel residence times are likely to approach much larger values than displayed, potentially exceeding the chemical lifetime for BVOCs with higher reactivities (e.g. $\tau_{\text{chem}} < 1$ h for the monoterpene myrcene, Fuentes et al. 2000).

The PDF of air-parcel residence times $p(\tau)$ is estimated from the LES results to better characterize the distribution of residence times as a function of release height (Fig. 5c). All the PDFs estimated from the LES display the power-law behaviour with a slope of approximately $-3/2$ as predicted by the theoretical model (Eq. 1). The simple theoretical model is capable of reproducing most of the features observed in the LES results (Fig. 5d). The main difference between the theoretical model and LES results is on the short time end of the PDFs, where the theoretical model tends to overestimate the probability of particles leaving the forest very quickly (Fig. 5b). This shortcoming of the theoretical model is consistent with the influence of

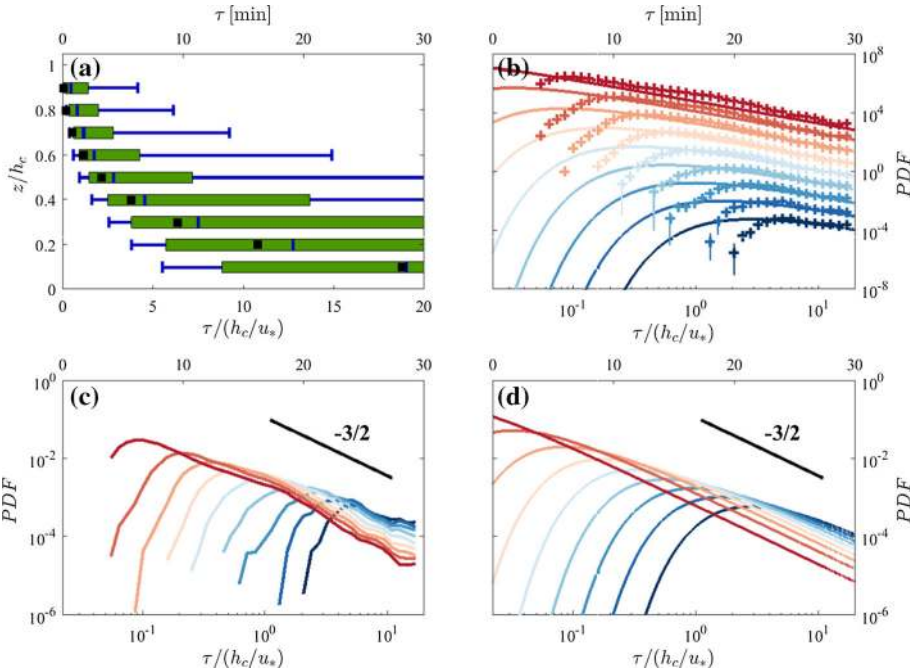

Fig. 5 Statistics of residence times for the Amazon rainforest case CTL. **a** Box-whisker plot of air-parcel residence times as a function of air-parcel release height for the control simulation. The median time is indicated with a *blue bar*, the *whiskers* indicate the 10th and 90th percentiles, while the *green box* corresponds to the inter-quartile range. Theoretical prediction for the median from Eq. 4 is indicated by *black squares*. **b** PDF of residence times as a function of air-parcel release height from the **c** LES results, and **d** theoretical model. Both results are overlaid for direct comparison in panel **b**, where results for different heights are vertically offset by an order of magnitude for improved readability. *Crosses* denote LES results, while the lines are the theoretical predictions. *Colors* indicate release height ranging from $z/h_c = 0.9$ (*dark red*) to $z/h_c = 0.1$ (*dark blue*)

near-field dispersion, which predominantly affects the PDF on short time scales, and cannot be approximated by a diffusion-like process (Taylor 1922), as assumed in the derivation of the model. In particular, the predominance of sweeps over ejections in the upper canopy (characterized by $S_{4,0}/S_{2,0}$ in Fig. 2d) will cause most air parcels to descend deeper into the canopy, increasing their residence time (this is consistent with the observed lowering of the particle-plume centreline near the source in the simulations of Pan et al. (2014a)). Note that this leads to an underestimation of the median residence time in the upper canopy by the theoretical model (Fig. 2a). Three levels of approximations are made in the theoretical model: (i) turbulent transport is expresented by an eddy diffusivity, (ii) the eddy diffusivity is parametrized through a simple equation, and (iii) an equivalent constant eddy diffusivity is adopted for each release height. Given these assumptions and the simplicity of the theoretical model, the overall agreement with the PDFs from the LES is satisfactory and is explored further in Sect. 4.4.

4.3 Effects of Canopy Structure and Turbulence Levels

Canopy structure strongly influences the residence times by altering the penetration and distribution of sweeps and ejections and the standard deviation of vertical velocity fluctuations

inside the canopy. Increases in LAI for simulation L30 to L90 show a consistent trend of increasing residence times caused by the decrease in penetration of mixing layer eddies and TKE inside the forest. Most of the changes occur for LAI varying from 3 to 6, and they become more pronounced for particles released deeper inside the canopy. This is seen as a spreading of the exponential tails in the PDFs between the cases L30 and L90 shown in Fig. 6a, c—note that the exponential increase in the PDFs for different release heights are farther apart for the L90 than they are for the L30 case. This effect is perhaps more clearly observed in the profiles of median residence times shown in Fig. 7b, where, similar to Bailey et al. (2014), the median time in the upper canopy is barely affected by the changes in LAI while a pronounced increase is observed deeper in the canopy.

The vertical distribution of LAI (i.e., the leaf-area-density profile) affects residence times in a slightly different way. Forests with large leaf area densities in the upper canopy (such as the cases $\beta 23$ and Bim) have a stronger predominance of sweeps over ejections in the upper canopy (Fig. 3d) resulting in longer residence times for parcels released in this region (Fig. 7). Conversely, the deeper penetration of sweeps in forests that have most of the leaf area in the lower canopy displaces air parcels released in the deeper canopy even closer to the ground surface, causing large residence times for releases in this region. Perhaps the main difference between the effects of LAI and canopy structure on residence times is that the latter can affect more strongly residence times in the upper canopy.

Residence times in the deep canopy are progressively reduced as turbulence levels increase (as measured by the value of u_* at the canopy top). The main effect of u_* is captured by simply scaling residence times by the canopy turnover time scale h_c/u_*. Thus, a rough approximation is that the effect of turbulence levels in the residence times is given by $\tau \propto u_*^{-1}$.

It is of interest to assess if the theoretical model is capable of capturing these strong effects of canopy structure and turbulence levels on the distribution of residence times. Overall, there is good agreement between the median residence times derived from the theoretical model and the LES (Fig. 8) for all cases, highlighting the theoretical model's ability to estimate residence times across a wide range of canopy structures, LAI and turbulence conditions. There is a slight, but systematic, underestimation of the median residence times (on average about 13%, as indicated by the linear fit shown in Fig. 8), which is clearly associated with the overestimation of $p(\tau)$ in the short time end of the PDF (i.e. in the portion of the PDF before its mode, which in the theoretical model is dominated by the exponential growth).

The largest errors are typically found for extreme conditions such as releases deep inside a forest with a large LAI. Note that the quality of the fit for parameter c_2 of the theoretical model (Table 2) is considerably worse for variations of canopy structure than for turbulence conditions and LAI. Nevertheless, the predicted median residence times of the theoretical model appear reasonable except for the lowermost level of case $\beta 23$.

4.4 Estimating Export Fractions of BVOCs

Given the reasonable capabilities of the simple theoretical model in capturing the details of the PDF of residence times under a wide range of conditions, it is of interest to compare export fractions of BVOCs predicted by the model with the usual empirical approach used in the MEGAN model. For the sake of generality, we make this comparison in a general framework, in terms of the Damköhler number as defined in Sect. 2.3. However, to make the comparison meaningful, typical model parameters representative of the Amazon forest environment are used. In particular, the canopy is represented by $LAI = 6$ and $h_c = 35$ m, and $c_2 = 0.53$ is adopted in the parametrization for the standard deviation of the vertical velocity (corresponding to the CTL case in Table 2). The BVOC source is restricted to the

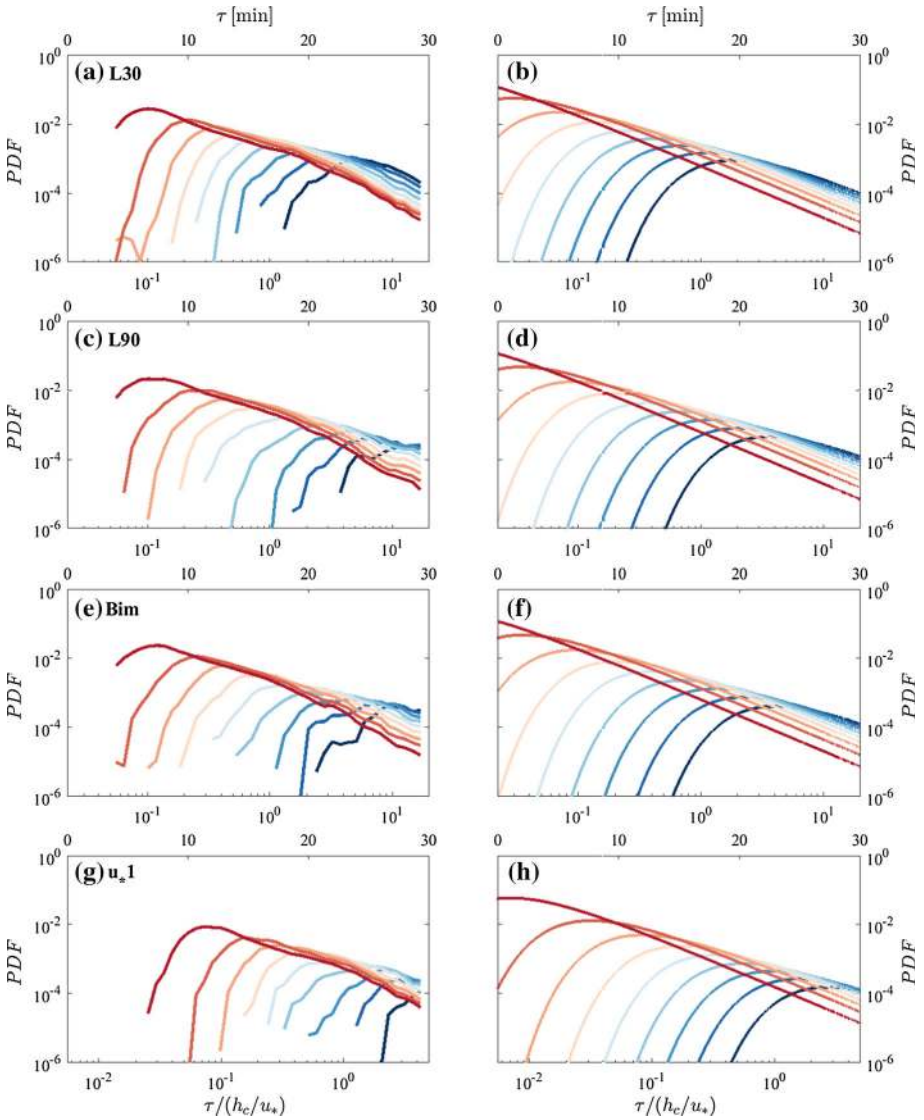

Fig. 6 PDF of residence times as a function of air-parcel release height from the LES results (**a**, **c**, **e**, **g**) and theoretical model (**b**, **d**, **f**, **h**) for simulations L30 (**a**, **b**), L90 (**c**, **d**), Bim (**e**, **f**), and u_*1 (**g**, **h**)

upper half of the canopy by setting $\alpha = 0.5$ and $\beta = (1 - \alpha) = 0.5$. Note that βh_c is the canopy depth excluding trunk space, which is assumed to be 2/3 for tropical forests in the MEGAN model. Since there was no apparent trunk space at the fieldsite and our calculations of BVOC emissions based on the relationships between leaf temperature, light and emissions (Guenther et al. 1995, 2006, 2012) indicate that the vast majority of BVOCs are emitted in the upper half of the canopy (not shown) α and β were changed from the default value.

The relevant range of Da was determined based on typical lifetimes of BVOCs and representative turbulent time scales for the Amazon forest. For the BVOC lifetimes, isoprene and

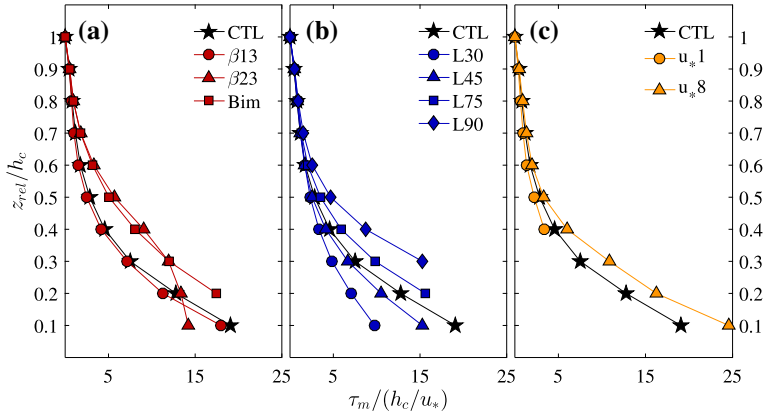

Fig. 7 Vertical distribution of normalized median air-parcel residence times $\tau_m/(h_c/u_*)$ for changes in **a** leaf area density, **b** LAI, and **c** friction velocity. See Table 1 for description of model runs

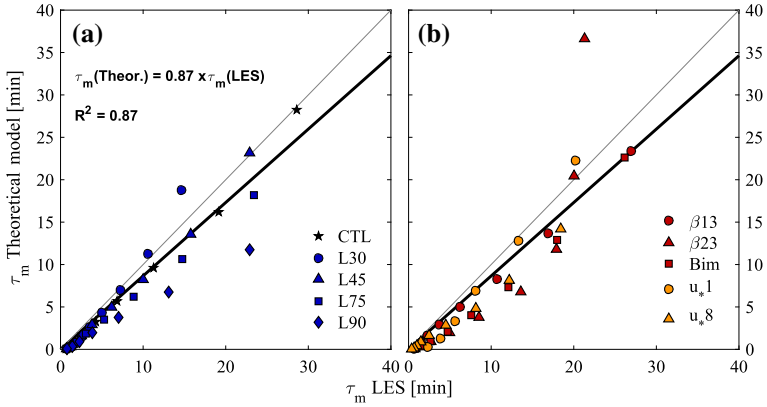

Fig. 8 Comparison of median air-parcel residence times (τ_m) derived from LES and theoretical model for z_{rel} between $0.1-0.9\,h_c$ using Eq. 4 for, **a** cases varying LAI, and **b** cases varying canopy structure and turbulence levels. The *black line* indicates the regression line calculated for all cases

the sesquiterpene β-caryophyllene were selected as examples of long- and short-lived BVOCs that are present in the Amazon forest. Lifetimes were estimated based on reactions with ozone and hydroxyl radical under typical unpolluted (10 ppb of ozone and 10^{12} radicals m^{-3} of hydroxyl radical) and polluted (50 ppb of ozone and 10^{13} radicals m^{-3} of hydroxyl radical) conditions. Finally, turbulence time scales were estimated for the extreme cases of $u_* = 0.1\,\mathrm{m\,s^{-1}}$ and $u_* = 0.8\,\mathrm{m\,s^{-1}}$. The resulting ranges of Da are displayed as coloured boxes in Fig. 9, and suggest that conditions in the Amazon forest can span over three orders of magnitude ($4 \times 10^{-3} < Da < 6$).

Five different model predictions are compared in Fig. 9:

1. Full model – prediction from the full theoretical model obtained by numerically integrating Eq. 17 using Eq. 15 and the eddy-viscosity model given by Eqs. 7 and 8.
2. Bulk model – prediction from the simplified theoretical model given by Eq. 18 with $G(LAI, \alpha = 0)$, which is equivalent to using the constant eddy diffusivity given by Eq. 9.

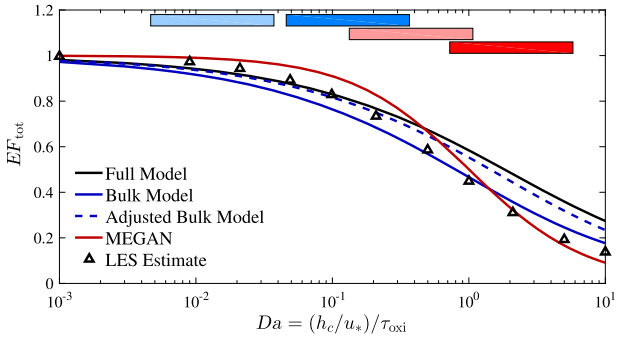

Fig. 9 Comparison of export fractions predicted by model included in the MEGAN model (*red line*), by the new theoretical model (*blue* and *black lines*), and estimates from the LES (*black triangles*) for a wide range of Damköhler numbers (Da) relevant to oxidation of BVOCs in the Amazon rainforest. *Coloured rectangles* represent typical ranges of Da for isoprene (*blue*) and β-caryophyllene (*red*) for unpolluted (*lighter shading*) and polluted (*darker shading*) conditions. See text for more details

3. Adjusted bulk model – prediction from the simplified theoretical model given by Eq. 18 with $G(LAI, \alpha = 0.5)$, which is equivalent to using the constant eddy diffusivity given by Eq. 19.
4. MEGAN – prediction from the empirical model used in the MEGAN model and given by Eq. 21.
5. LES estimate – prediction obtained by integrating $\int_0^\infty p_{LES}(\tau; z_{rel}) \exp(\tau/\tau_{oxi}) d\tau$ numerically. Here, $p_{LES}(\tau; z_{rel})$ is the PDF obtained from the LES results for the CTL case extended beyond 30 min by assuming a continuation of the $\tau^{-3/2}$ decay. For consistency with the other model predictions, only results for release heights $z_{rel} > 0.5\, h_c$ were used (equivalent to $\alpha = 0.5$).

In interpreting Fig. 9, the LES results are considered to be the most reliable estimates as they do not rely on any assumptions about vertical transport within the canopy. When compared to LES results, the performance of the empirical model proposed for the MEGAN model in Guenther et al. (2006) is surprisingly good: the empirical model overestimates export fractions for $Da < 1$ and overestimates it for $Da > 1$, but the differences are never much larger than about 10%. The new theoretical model has improved performance over MEGAN for $Da < 0.5$ (corresponding to the isoprene range for the Amazon), but it significantly overestimates export fractions for $Da > 0.5$ (corresponding to most of the β-caryophyllene range for the Amazon). This overprediction in export fractions for highly reactive gases is clearly associated with the overestimation of the PDF for shorter residence times, as this region of the PDF becomes increasingly more important in determining the total export fraction for large Da. Comparison between the full model and the two bulk models suggests that the performance of the bulk model is comparable to that of the full modelling approach if the constant eddy diffusivity is determined only based on the region where the source of BVOCs is active (in this case in the range $1/2 \leq z/h_c \leq 1$). Note that the full model requires two numerical integrations (in Eqs. 8, 17), and not much accuracy in the final export fraction is lost by a replacing this by a simpler analytical bulk model.

The deviation between LES estimates, the MEGAN empirical model, and theoretical models developed here highlight the challenges that arise from representing canopy transport time scales over the entire canopy through a single relationship. It is not possible at this point to indicate which model provides a better representation of the export fractions in the

Amazon forest, as it is difficult to quantify export fractions from measurements, and the LES results are accurate in vertical transport but still rely on oversimplified chemistry. Perhaps, more important than the differences between modelling approaches, is the overall result that suggests that the export fraction of BVOCs in the Amazon forest may vary between almost 100% for isoprene under unpolluted and windy conditions and less than 20% for reactive sesquiterpenes under polluted and calm conditions.

As a final note, none of the models discussed here includes the possible effects of air parcels re-entering the canopy and transporting BVOCs back into the canopy. Including these effects greatly increases the complexity of the problem, as the mixing ratios of BVOCs in these air parcels are affected by vertical mixing and chemistry within the ABL. This coupling between the canopy and ABL warrants further research.

5 Summary and Conclusions

The present study shows that for dense and tall forests it is necessary to include the effect of air-parcel residence time when estimating the out-of-canopy export of plant-emitted and reactive hydrocarbons. Because estimation of residence times requires three-dimensional information of the flow field within the canopy (which cannot be readily obtained from field measurements), canopy-resolving numerical simulations using the LES technique are the most reliable source of information. Air-parcel residence times obtained from LES show strong variability in response to parcel origin within the canopy, leaf-area-density profiles, and turbulence levels. As an example, the modelled median air-parcel residence times within the forest canopy can range from seconds in the forest crown to approximately 30 min in the lower canopy. In the lower forest canopy, the distribution of residence times is strongly skewed towards longer residence times, thus providing ample time for chemical reactions to occur before air parcels leave the forest. While median or mean residence times cannot properly characterize the distribution of canopy air-parcel residence times, they can be used to support the notion that in-canopy chemical reactions are important to consider in the estimation of ecosystem-level BVOC fluxes. Median air-parcel residence times near the forest floor ($\approx$30 min) are comparable to the lifetimes of some forest-emitted hydrocarbons for reactions with O_3 and OH, resulting in reduced BVOC canopy export fractions.

We propose a new theoretical model to predict the probability density function (PDF) of air-parcel residence times within plant canopies based on the Fokker–Planck equation. The PDFs predicted by the model are in very good agreement with those obtained from LES for a range of canopy architectures, except that they overpredict the probability of particles leaving the canopy in very short times. This is consistent with the lack of treatment of near-field (non-diffusive) processes, but could also be caused by other effects not included in the theory (one clear example being the mean drift associated with large vertical gradients in eddy diffusivity). Overall, the proposed model is valuable in estimating air-parcel residence times, and the main limitations are associated with air parcels that originate from deep inside the canopy. The main predictions (Eqs. 1, 4, 5) require only information on canopy height and a model of the eddy diffusivity inside the canopy. We developed one simple model for the eddy diffusivity here that requires further specification of the friction velocity at canopy top and the use of an empirical parameter to describe the vertical profile of vertical velocity variance inside the canopy. A good model for σ_w is needed for reliable prediction of the PDFs of residence times to be possible. Thus, whenever observations data are available, the model for $\sigma_w(z)$ should be adjusted either by fitting a new constant c_2 or by making changes

to the functional dependence of σ_w on z if needed. Even though only neutral stratification is considered in the present work, non-neutral conditions would require major changes to $\sigma_w(z)$ and $T_L(z)$. Therefore, by invoking models for $\sigma_w(z)$ and $T_L(z)$ that include effects of atmospheric stability, it might be possible to extend the model to stable and unstable conditions.

Motivated by the need to have a simple method to determine the in-canopy chemical destruction of plant-emitted hydrocarbons, a simple chemical model, assuming first-order chemical kinetics, is included in the theoretical model, yielding predictions of out-of-canopy export fractions of unreacted hydrocarbons as a function of the Damköhler number. Model predictions for the Amazon forest are compared to those obtained by the empirical parametrization proposed as part of the MEGAN model and results inferred from LES. At the moment, it is not possible to assert which modelling framework is the most reliable. Field observations and/or canopy-resolving LES fully coupled with a more complete chemical mechanism are needed to help elucidate this issue.

Acknowledgements The authors acknowledge partial funding from DOE through the Office of Biological and Environmental Research (BER) Atmospheric Systems Research (ASR) program (DE-SC0011075). We thank the anonymous reviewers for their helpful comments.

Appendix 1: The First Passage Solution

If the turbulent transport of air parcels is assumed to be diffusive with a constant eddy diffusivity K_{eq}, then the time evolution of the particle position can be modelled by a Wiener process without mean drift

$$\mathrm{d}z = \sqrt{2K_{\mathrm{eq}}}\mathrm{d}W, \tag{24}$$

where W is a Wiener process with independent Gaussian increments. Under these conditions, the time evolution of the probability density function (PDF) of the particle position satisfies the Fokker–Planck equation (Thomson 1987; Rodean 1996)

$$\frac{\partial P(z,t;z_{\mathrm{rel}})}{\partial t} = K_{\mathrm{eq}}\frac{\partial^2 P(z,t;z_{\mathrm{rel}})}{\partial z^2}, \tag{25}$$

where $P(z,t;z_{\mathrm{rel}})$ is the probability of a particle released at $z = z_{\mathrm{rel}}$ at $t = 0$ to be found at z at a time t. Considering a semi-infinite domain (i.e., $z < h_c$), the first time a parcel crosses the boundary can be modelled by placing an absorbing boundary at $z = h_c$. Thus, the two boundary conditions for Eq. 25 are given by $P(z = h_c, t; z_{\mathrm{rel}}) = 0$ and $P(z \to -\infty, t; z_{\mathrm{rel}}) = 0$. Together with the initial condition $P(z, t = 0; z_{\mathrm{rel}}) = \delta(z - z_{\mathrm{rel}})$, the solution is the well-known Gaussian function

$$P(z,t;z_{\mathrm{rel}}) = \frac{1}{\sqrt{4\pi K_{\mathrm{eq}}}}t^{-1/2}\left\{\exp\left[-\frac{(z-z_{\mathrm{rel}})^2}{4K_{\mathrm{eq}}t}\right] - \exp\left[-\frac{(z-(2h_c-z_{\mathrm{rel}}))^2}{4K_{\mathrm{eq}}t}\right]\right\} \tag{26}$$

In the present case, the probability of an air parcel still being in the domain $z < h_c$ (i.e., it has not crossed the boundary yet) is given by

$$F(t;z_{\mathrm{rel}}) = \int_{z=0}^{\infty} P(z,t;z_{\mathrm{rel}})\mathrm{d}z = \mathrm{erf}\left(\frac{h_c - z_{\mathrm{rel}}}{\sqrt{4K_{\mathrm{eq}}t}}\right) \tag{27}$$

The probability $F(t;z_{\mathrm{rel}})$ is usually referred to as the survival probability. The rate of decrease in $F(t;z_{\mathrm{rel}})$ at a given time τ is equal to the probability of particles crossing the

boundary at that time. Thus, the first-passage distribution for the present scenario is given by

$$p(\tau; z_{\text{rel}}) = -\left.\frac{\partial F(t; z_{\text{rel}})}{\partial t}\right|_{z=h_c, t=\tau} = \frac{(h_c - z_{\text{rel}})}{\sqrt{4\pi K_{\text{eq}}}}\tau^{-3/2}\exp\left[-\frac{(h_c - z_{\text{rel}})^2}{4K_{\text{eq}}\tau}\right], \quad (28)$$

which is identical to Eq. 1.

References

Bailey BN, Stoll R (2013) Turbulence in sparse, organized vegetative canopies: a large-eddy simulation study. Boundary-Layer Meteorol 147(3):369–400. doi:10.1007/s10546-012-9796-4

Bailey BN, Stoll R, Pardyjak ER, Mahaffee WF (2014) Effect of vegetative canopy architecture on vertical transport of massless particles. Atmos Environ 95:480–489. doi:10.1016/j.atmosenv.2014.06.058

Bou-Zeid E, Meneveau C, Parlange M (2005) A scale-dependent Lagrangian dynamic model for large eddy simulation of complex turbulent flows. Phys Fluids 17(2):025,105. doi:10.1063/1.1839152

Canuto C, Hussaini MY, Quarteroni AM, Zang TA Jr (2012) Spectral methods in fluid dynamics. Springer Science & Business Media, Dordrecht, 568 pp

Cescatti A, Marcolla B (2004) Drag coefficient and turbulence intensity in conifer canopies. Agric Forest Meteorol 121(3–4):197–206. doi:10.1016/j.agrformet.2003.08.028

Chamecki M, Meneveau C, Parlange MB (2008) A hybrid spectral/finite-volume algorithm for large-eddy simulation of scalars in the atmospheric boundary layer. Boundary-Layer Meteorol 128(3):473–484. doi:10.1007/s10546-008-9302-1

Chamecki M, Meneveau C, Parlange MB (2009) Large eddy simulation of pollen transport in the atmospheric boundary layer. J Aerosol Sci 40(3):241–255. doi:10.1016/j.jaerosci.2008.11.004

Coppin PA, Raupach MR, Legg BJ (1986) Experiments on scalar dispersion within a model plant canopy part II: An elevated plane source. Boundary-Layer Meteorol 35(1–2):167–191. doi:10.1007/BF00117307

Cox D, Miller H (1965) The theory of stochastic processes. Methuen's monographs on applied probability and statistics. Methuen, London, 398 pp

Damköhler G (1940) Der Einfluss der Turbulenz auf die Flammengeschwindigkeit in Gasgemischen (in German). Z Electrochem Angewand Physikal Chem 46:601–626

Dannon HV (2011) Power means calculus and fractional calculus. Gauge Institute, Minneapolis, 119 pp

Denmead OT, Bradley EF (1985) Flux-gradient relationships in a forest canopy. In: Hutchison BA, Hicks BB (eds) The Forest-Atmosphere Interaction. Springer, Netherlands pp 421–442, doi:10.1007/978-94-009-5305-5_27

Dupont S, Patton EG (2012) Influence of stability and seasonal canopy changes on micrometeorology within and above an orchard canopy: The CHATS experiment. Agric Forest Meteorol 157:11–29. doi:10.1016/j.agrformet.2012.01.011

Edburg SL, Stock D, Lamb BK, Patton EG (2012) The effect of the vertical source distribution on scalar statistics within and above a forest canopy. Boundary-Layer Meteorol 142(3):365–382. doi:10.1007/s10546-011-9686-1

Finlayson-Pitts BJ (2000) Chemistry of the upper and lower atmosphere: theory, experiments, and applications. Academic Press, San Diego, 969 pp

Finnigan J (2000) Turbulence in plant canopies. Annu Rev Fluid Mech 32(1):519–571

Foken T, Göckede M, Mauder M, Mahrt L, Amiro B, Munger W (2004) Post-field data quality control. In: Lee X, Massman W, Law B (eds) Handbook of micrometeorology. Springer, Dordrecht, pp 181–208

Freire LS, Gerken T, Ruiz-Plancarte J, Wei D, Fuentes JD, Katul G, Dias N, Acevedo O, Chamecki M (2016) Turbulent mixing and removal of ozone within an Amazon rainforest canopy. J Geophys Res. doi:10.1002/2016JD026009

Fuentes JD, Gu L, Lerdau M, Atkinson R, Baldocchi D, Bottenheim JW, Ciccioli P, Lamb B, Geron C, Guenther A, Sharkey TD, Stockwell W (2000) Biogenic hydrocarbons in the atmospheric boundary layer: a review. Bull Am Meteorol Soc 81(7):1537–1575. doi:10.1175/1520-0477(2000)081<1537:BHITAB>2.3.CO;2

Fuentes JD, Wang D, Bowling DR, Potosnak M, Monson RK, Goliff WS, Stockwell WR (2007) Biogenic hydrocarbon chemistry within and above a mixed deciduous forest. J Atmos Chem 56(2):165–185. doi:10.1007/s10874-006-9048-4

Fuentes JD, Chamecki M, Nascimento dos Santos RM, Von Randow C, Stoy PC, Katul G, Fitzjarrald D, Manzi A, Gerken T, Trowbridge A, Freire LS, Ruiz-Plancarte J, Furtunato Maia JM, Tota J, Dias N, Fisch G,

Schumacher C, Acevedo O, Mercer JR (2016) Linking meteorology, turbulence, and air chemistry in the Amazon rainforest. Bull Am Meteorol Soc 97:2329–2342. doi:10.1175/BAMS-D-15-00152.1
Guenther A, Hewitt CN, Erickson D, Fall R, Geron C, Graedel T, Harley P, Klinger L, Lerdau M, Mckay WA, Pierce T, Scholes B, Steinbrecher R, Tallamraju R, Taylor J, Zimmerman P (1995) A global model of natural volatile organic compound emissions. J Geophys Res 100(D5):8873–8892. doi:10.1029/94JD02950
Guenther A, Karl T, Harley P, Wiedinmyer C, Palmer PI, Geron C (2006) Estimates of global terrestrial isoprene emissions using MEGAN (Model of Emissions of Gases and Aerosols from Nature). Atmos Chem Phys 6(11):3181–3210. doi:10.5194/acp-6-3181-2006
Guenther AB, Jiang X, Heald CL, Sakulyanontvittaya T, Duhl T, Emmons LK, Wang X (2012) The Model of Emissions of Gases and Aerosols from Nature version 2.1 (MEGAN2.1): an extended and updated framework for modeling biogenic emissions. Geosci Model Dev 5(6):1471–1492. doi:10.5194/gmd-5-1471-2012
Hamba F (1993) A modified K model for chemically reactive species in the planetary boundary layer. J Geophys Res Atmos 98(D3):5173–5182
Horst T, Semmer S, Maclean G (2015) Correction of a non-orthogonal, three-component sonic anemometer for flow distortion by transducer shadowing. Boundary-Layer Meteorol 155(3):371–395
Iwata H, Harazono Y, Ueyama M (2010) Influence of source/sink distributions on flux-gradient relationships in the roughness sublayer over an open forest canopy under unstable conditions. Boundary-Layer Meteorol 136(3):391–405. doi:10.1007/s10546-010-9513-0
Jardine K, Yañez Serrano A, Arneth A, Abrell L, Jardine A, van Haren J, Artaxo P, Rizzo LV, Ishida FY, Karl T, Kesselmeier J, Saleska S, Huxman T (2011) Within-canopy sesquiterpene ozonolysis in Amazonia. J Geophys Res 116(D19):301. doi:10.1029/2011JD016243
Kaimal JC, Finnigan JJ (1994) Atmospheric boundary layer flows: their structure and measurement. Oxford University Press, New York, 304 pp
Katul GG, Mahrt L, Poggi D, Sanz C (2004) One-and two-equation models for canopy turbulence. Boundary-Layer Meteorol 113(1):81–109
Katul GG, Poporato A, Nathan R, Siqueira M, Soons M, Poggi D, Horn H, Levin S (2005) Mechanistic analytical models for long-distance seed dispersal by wind. Am Natural 166(3):368–381
Marques Filho AdO, Dallarosa RG, Pacheco VB (2005) Radiação solar e distribuição vertical de área foliar em floresta—Reserva Biológica do Cuieiras - ZF2, Manaus (in Portuguese). Acta Amazon 35(4):427–436
Massman W, Weil J (1999) An analytical one-dimensional second-order closure model of turbulence statistics and the lagrangian time scale within and above plant canopies of arbitrary structure. Boundary-Layer Meteorol 91(1):81–107
McWilliam AL, Roberts J, Cabral O, Leitao M, De Costa A, Maitelli G, Zamparoni C (1993) Leaf area index and above-ground biomass of terra firme rain forest and adjacent clearings in Amazonia. Funct Ecol 7:310–317
Pan Y, Chamecki M (2016) A scaling law for the shear-production range of second-order structure functions. J Fluid Mech 801:459–474
Pan Y, Chamecki M, Isard SA (2014) Large-eddy simulation of turbulence and particle dispersion inside the canopy roughness sublayer. J Fluid Mech 753:499–534. doi:10.1017/jfm.2014.379
Pan Y, Follett E, Chamecki M, Nepf H (2014b) Strong and weak, unsteady reconfiguration and its impact on turbulence structure within plant canopies. Phys Fluids 26(10):105,102. doi:10.1063/1.4898395
Patton EG, Davis KJ, Barth MC, Sullivan PP (2001) Decaying scalars emitted by a forest canopy: a numerical study. Boundary-Layer Meteorol 100(1):91–129
Patton EG, Sullivan PP, Shaw RH, Finnigan JJ, Weil JC (2016) Atmospheric stability influences on coupled boundary layer and canopy turbulence. J Atmos Sci 73(4):1621–1647
Peyret R, Taylor TD (2012) Computational methods for fluid flow. Springer Science & Business Media, New York, 358 pp
Queck R, Bienert A, Maas HG, Harmansa S, Goldberg V, Bernhofer C (2011) Wind fields in heterogeneous conifer canopies: parameterisation of momentum absorption using high-resolution 3D vegetation scans. Eur J Forest Res 131(1):165–176. doi:10.1007/s10342-011-0550-0
Raupach M (1989) Applying lagrangian fluid mechanics to infer scalar source distributions from concentration profiles in plant canopies. Agric Forest Meteorol 47(2–4):85–108
Raupach MR, Finnigan JJ, Brunei Y (1996) Coherent eddies and turbulence in vegetation canopies: the mixing-layer analogy. Boundary-Layer Meteorol 78(3–4):351–382. doi:10.1007/BF00120941
Redner S (2001) A guide to first passage processes. Cambridge University Press, Cambridge, 312 pp
Rinne J, Taipale R, Markkanen T, Ruuskanen TM, Hellen H, Kajos MK, Vesala T, Kulmala M (2007) Hydrocarbon fluxes above a Scots pine forest canopy: measurements and modeling. Atmos Chem Phys 7(12):3361–3372. doi:10.5194/acp-7-3361-2007

Rinne J, Markkanen T, Ruuskanen TM, Petäjä T, Keronen P, Tang M, Crowley JN, Rannik Ü, Vesala T (2012) Effect of chemical degradation on fluxes of reactive compounds—a study with a stochastic Lagrangian transport model. Atmos Chem Phys 12(11):4843–4854. doi:10.5194/acp-12-4843-2012

Rodean HC (1996) Stochastic Lagrangian models of turbulent diffusion, Meteorological Monographs, vol 48. American Meteorological Society, Boston

Schrödinger E (1915) Zur Theorie der Fall- und Steigversuche an Teilchen mit Brownscher Bewegung. Physikal Z 16:289–295

Shaw RH, Schumann U (1992) Large-eddy simulation of turbulent flow above and within a forest. Boundary-Layer Meteorol 61(1–2):47–64. doi:10.1007/BF02033994

Strong C, Fuentes JD, Baldocchi D (2004) Reactive hydrocarbon flux footprints during canopy senescence. Agric Forest Meteorol 127(3–4):159–173. doi:10.1016/j.agrformet.2004.07.011

Stroud C, Makar P, Karl T, Guenther A, Geron C, Turnipseed A, Nemitz E, Baker B, Potosnak M, Fuentes JD (2005) Role of canopy-scale photochemistry in modifying biogenic-atmosphere exchange of reactive terpene species: Results from the CELTIC field study. J Geophys Res 110(D17):303. doi:10.1029/2005JD005775

Taylor GI (1922) Diffusion by continuous movements. Proc Lond Math Soc 20(1):196–212

Thomson DJ (1987) Criteria for the selection of stochastic models of particle trajectories in turbulent flows. J Fluid Mech 180:529–556. doi:10.1017/S0022112087001940

Tóta J, Fitzjarrald DR, da Silva Dias MAF (2012) Amazon rainforest exchange of carbon and subcanopy air flow: Manaus LBA Site—a complex terrain condition. Sci World J 2012:1–19. doi:10.1100/2012/165067

Yee E, Wilson JD (2007) Instability in Lagrangian stochastic trajectory models, and a method for its cure. Boundary-Layer Meteorol 122:243–261. doi:10.1007/s10546-006-9111-3

Weil JC, Sullivan PP, Moeng CH (2004) The use of large-eddy simulations in Lagrangian particle dispersion models. J Atmos Sci 61(23):2877–2887. doi:10.1175/JAS-3302.1